



Transactions, SMiRT-26
Berlin/Potsdam, Germany, July 10-15, 2022
Division II

PIPE ELBOW STRUCTURAL INTEGRITY ASSESSMENT METHOD FOR R6

Yuebao Lei¹

¹ Dr, EDF Energy Nuclear Generation Ltd, Barnett Way, Barnwood, Gloucester, GL4 3RS, United Kingdom (yuebao.lei@edf-energy.com)

ABSTRACT Recently, guidance has been developed for fracture assessment of defective elbows using the R6 procedure. This paper provides an overview of the newly-developed guidance and supporting validation. The guidance is validated using 75 cases of 3-D finite element (FE) elastic-plastic J results, for smooth elbows of various geometries with axial/circumferential internal/external semi-elliptical/extended/fully-circumferential surface cracks under internal pressure, in-plane/out-of-plane bending moment, torsion and various load combinations, by comparing the FE-based Option 3 failure assessment curves (FAC) with the R6 Option 2 FAC. The results show that, for 74 out of 75 cases, the FE-based Option 3 data points are above the R6 Option 2 FAC with reasonable conservatism when the guidance for evaluating the elbow stress intensity factor and limit load is followed. In other words, following the new guidance can lead to reasonably conservative assessment results.

INTRODUCTION

Pipe elbows are widely used in nuclear power plants, both in nuclear and conventional islands. Structural integrity assessments of pipe elbows with detected or postulated defects are required to support structural integrity-related safety cases and plant life extension arguments. Recently, guidance has been developed (Lei 2020b) for fracture assessment of defective elbows using the R6 procedure (R6 2019) after years of investigation. This paper provides an overview of the newly-developed guidance for structural integrity assessment of defective elbows using R6 and its validation. The new guidance is intended to be included in an upcoming revision of the R6 procedure.

The R6 procedure (R6 2019) uses a J -based failure assessment diagram (FAD) method to assess defective components against fracture and plastic collapse. When performing an assessment using the R6 procedure, the most important two parameters, L_r and K_r , should be evaluated, which are defined as follows.

$$L_r = P/P_L = \sigma_{\text{ref}}/\sigma_y \quad (1)$$

$$K_r = (K_I^p + VK_I^s)/K_{\text{mat}} \quad (2)$$

In Eqn. (1), P is the applied primary load, in general, and P_L is the corresponding limit load for the defective component under the load type P . L_r can alternatively be defined as the ratio between the reference stress, σ_{ref} , and σ_y , where σ_y is the yield stress or 0.2% plastic strain off-set stress of the material. Equation (1) also defines the relationship between the reference stress and limit load. In Eqn. (2), K_I^p and K_I^s are the stress intensity factors (SIF) of the defective component for primary and secondary load, respectively, and V is a plasticity correction factor for secondary load, which is defined in R6 (R6 2019). In an assessment, the assessment point (L_r , K_r) is marked on the selected FAD. The assessment result is “acceptable” if the assessment point is located inside the area surrounded by the failure assessment curve (FAC), the cut-off line $L_r = L_r^{\text{max}}$ (where $L_r^{\text{max}} \geq 1$ is the ratio between the flow stress and σ_y) and the L_r , K_r axes. Of course, the assessment margin should also satisfy the requirement of the case in an assessment of real component. It is clear that the limit load and SIF solutions are two key parameters to evaluate L_r and K_r . Note that the

limit load used in fracture assessment should lead to conservative predictions of J and plastic collapse. The new guidance for defective pipe elbow assessment recommends validated SIF and global/local limit load solutions.

OVERVIEW OF THE GUIDANCE

The general guidance in R6 (R6 2019) should be followed when performing defect assessments for pipe elbows. Guidance given in this paper is for evaluating the required SIF and limit load.

Elbow Geometry and Loads

This guidance is for defects in smooth pipe elbows with attached straight pipes at the two ends. The dimensions of a pipe elbow can be described by its elbow radius, R_c , elbow angle, ψ_c , pipe mean radius, r_m , and pipe wall-thickness, t (see Fig. 1). For elbows with uneven pipe thickness, the minimum thickness should be used in assessments. The elbow factor, λ_b , is defined as

$$\lambda_b = (R_c/r_m)/(r_m/t) \quad (3)$$

The elbow factor, λ_b , ratios R_c/r_m and r_m/t , and elbow angle, ψ_c , are four important parameters to define a pipe elbow. When required, the inner and outer radii of the pipe (r_i and r_o , respectively) may be obtained from r_m and t as $r_i = r_m - t/2$ and $r_o = r_m + t/2$. The load types considered in the guidance are internal pressure, p , in-plane bending moment, M_2^0 , out-of-plane bending moment, M_3^0 , and torsion moment, M_1^0 . Figure 1 shows the coordinate system (1, 2, 3) and the positive directions of the moments. The moment loads are assumed to be transferred to the elbow body through the attached straight pipes.

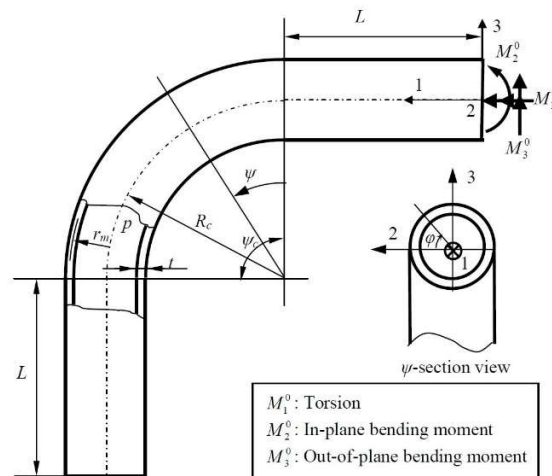


Figure 1 Definition of elbow geometry parameters and loads

Defect Types

The defects which can be assessed are those which can be characterised as internal/external semi-elliptical or fully-circumferential surface cracks, and internal/external semi-elliptical or extended axial surface cracks. Through-wall cracks are not yet included and corresponding guidance will be developed later.

The crack location in the elbow is defined by two angular parameters, ψ and ϕ (see Fig. 1). A crack can be located at any of the locations defined by $0 \leq \psi \leq \psi_c$ ($\psi = 0$ and $\psi = \psi_c$ correspond to the intersections between the elbow and the attached straight pipes) and $\pi \geq \phi > -\pi$ ($\phi = \pi/2$ for extrados cracks, $\phi = -\pi/2$ for intrados cracks and $\phi = 0$ and π for crown cracks).

Stress Intensity Factor

The SIF may be calculated using the detailed elastic FE method or evaluated using the solutions given in Lei and Budden (2017) by following the guidance given in Appendix C, ‘Guidance for SIF calculation of defective elbows’, and Appendix A, ‘Guidance for elbow stress calculation in evaluation of SIF’, in Lei (2017). Note that the SIF estimation method given in Lei and Budden (2017) is based on the uncracked-body through-thickness elastic stress distribution at the crack location. Therefore, the method can also be used to estimate the SIF for secondary stresses. It is intended that the SIF solutions given in Lei and Budden (2017) and guidance in Lei (2017) will be included in the SIF compendium of R6 Section IV.3 in an upcoming revision of the R6 procedure.

Limit Load Solutions

The following global and local limit load solutions are recommended for use in assessments of power station elbows. The global limit load solutions should be used first, or the local limit load if a proper global limit load solution is unavailable.

The recommended global and local limit loads have been validated (Lei (2020b)) based on the FE J database, for $R_c/r_m = 1.96 \sim 6$ and $\lambda_b = 0.146 \sim 0.84$, but they are judged to be valid for $R_c/r_m \geq 1.96$ and $\lambda_b \geq 0.1$. These limit load solutions are intended to be included in an upcoming revision of the R6 procedure.

Global limit load solutions

The six global limit load solutions given in Lei (2021) (see also Lei and Budden (2022)) are recommended, including

- Circumferential internal/external surface cracks under pressure
- Circumferential internal/external surface cracks under a bending moment
- Circumferential internal/external surface cracks under combined pressure and moment
- Circumferential internal/external surface cracks under combined pressure and torsion
- Circumferential internal/external cracks under combined bending moment and torsion
- Axial internal/external surface cracks under pressure

Local limit load

The recommended local limit load for short surface cracks is based on a local limit load model developed by Lei (2020a) for shell/plate type components (plane stress conditions along the thickness) with surface cracks. The model (Fig. 2(a)) is a plate of width $2D$, which contains a rectangular surface crack of depth a and length $2c$ circumscribing the real surface defect, and has the same thickness, t , as the component at the crack location. The plate is assumed to be sufficiently long (this could be different from the real structure to be simulated). The half width of the plate, D , is defined as

$$D = (k_0 + k(a/t))c < W \quad (4)$$

For defective pipe elbows, $k_0 = 1.7$ and $k = 1$ for circumferential surface cracks and $k_0 = 3$ and $k = 1$ for axial surface cracks. In Eqn. (4), the calculated D should not exceed the real elbow dimension, W , measured in the defect section. W is the half circumference of the elbow pipe for circumferential defects and the shorter of the two distances from the centre of the defect to the ends of attached straight pipes for axial defects.

The recommended local limit load for long surface cracks, including fully-circumferential surface cracks and extended axial surface cracks, is based on the same plate model as for short surface cracks but with an extended surface crack of depth a (see Fig. 2(b)). For this model, $D = c$ and the absolute value of the plate width $2D$ has no effect on the limit load because of the plane stress assumption along the plate width. Therefore, the plate width $2D$ is assumed to be unity. The rotation of the plate ends is restricted to reduce conservatism for deep cracks.

The model plates are remotely loaded by the primary stresses of the component at the crack location obtained from elastic uncracked-body stress analysis using the elastic FE method or the simplified stress

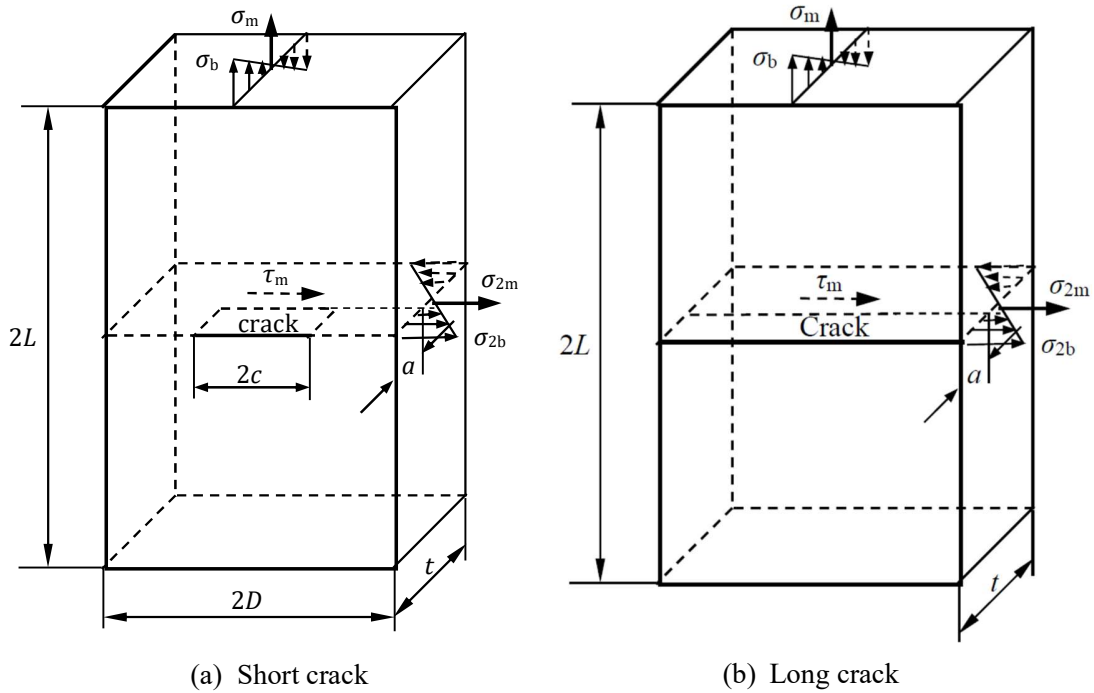


Figure 2 Local limit load models

solutions given in Marie et al. (2007). The stresses obtained from the elastic stress analysis should be expressed as the membrane stress, σ_m , and through-thickness bending stress, σ_b , normal to the crack plane, the membrane stress, σ_{2m} , and the bending stress, σ_{2b} , parallel to the crack plane and the average shear stress in the crack plane, τ_m . The through-thickness bending stresses, σ_b and σ_{2b} , are positive if the bending stresses tend to stretch the front surface containing the crack. A negative σ_m or σ_b should be set to zero when evaluating the limit load. For defects located at or close to the intersection between the pipe bend and the attached straight pipe, stress analysis for the straight pipe (without a connection to the bend) should also be performed under the same loading conditions. The maximum σ_m value obtained from the two analyses together with other stress components from the pipe elbow analysis should be used in the assessment.

The reference stress from the models is then expressed as

$$\sigma_{\text{ref}} = \sqrt{(3\tau_m^2 + (\sigma_{\text{ref}})_{\tau_m=0}^2)} \quad (5)$$

where the reference stress without shear stress, $(\sigma_{\text{ref}})_{\tau_m=0}$, and the stress ratio, λ_{bt} , are defined in Eqns. (6) and (7) below.

$$(\sigma_{\text{ref}})_{\tau_m=0} = (\sigma_{\text{ref}})_{\text{npb}} \sqrt{1 - 0.5\lambda_{bt} + \lambda_{bt}^2} \quad (6)$$

$$\lambda_{bt} = \frac{2}{3} \frac{\sigma_{2b}}{(\sigma_{\text{ref}})_{\text{npb}}} \quad (7)$$

The reference stress without the bending stress parallel to the crack plane, $(\sigma_{\text{ref}})_{\text{npb}}$, in Eqns. (6) and (7) is defined for short and long surface cracks in Eqns. (8) and (10) below, respectively.

For short surface cracks ($c \leq 4t$),

$$(\sigma_{\text{ref}})_{\text{npb}} = \begin{cases} \frac{\sigma_m}{n_L(a/t, c/D, \lambda, \lambda_1)} & \text{for } \sigma_m \neq 0 \\ \frac{2}{3} \frac{\sigma_b}{m_L(a/t, c/D, \lambda_2)} & \text{for } \sigma_m = 0 \end{cases} \quad (8)$$

where n_L and m_L are the normalised limit membrane stress and limit bending stress, respectively, under combined loading, which can be calculated using the solutions developed by Lei and Budden (2015). The load ratios, λ , λ_1 and λ_2 in Eqn. (8) are defined by

$$\lambda = \frac{\sigma_b}{6\sigma_m}, \quad \lambda_1 = \frac{\sigma_{2m}}{\sigma_m}, \quad \lambda_2 = \frac{\sigma_{2m}}{\sigma_b} \quad (9)$$

For long surface cracks ($c > 4t$),

$$(\sigma_{\text{ref}})_{\text{npb}} = \sqrt{\frac{3}{4}\sigma_{2m}^2 + \frac{1}{(1-a/t)^4} \left(\frac{|\sigma_b|}{3} + \sqrt{\left(\frac{\sigma_b}{3}\right)^2 + (1-a/t)^4 \left(\frac{\sigma_m}{(1-a/t)} - \frac{\sigma_{2m}}{2}\right)^2} \right)^2} \quad (10)$$

The reference stress obtained from Eqn. (5) is then used to define L_r via Eqn. (1).

VALIDATION

In the R6 procedure (R6 2019), a J -based FAD method is used in fracture assessments, which is underpinned by the reference stress J -estimation scheme. Therefore, an assessment using the R6 FAD method is equivalent to a J prediction using the reference stress approach. This assessment method may be validated by comparing the FE J -based Option 3 failure assessment curve (FAC) and the material dependent Option 2 FAC or general Option 1 FAC. The assessment method is conservative if the Option 3 FAC is located above the Option 2 or Option 1 FAC for each case. Note that, in this way, the recommended SIF estimation and limit loads are validated because the estimated SIF and limit load should be used in constructing the FE J -based Option 3 FAC.

Available FE J data Used in Validation

Well-documented FE J results for defective elbows from two internal company reports, the “BENCH-KJ” report by Kayser (2016) and the Frazer Nash (FNC) report by O’Neill and Brett (2016) are used in this validation exercise. The 75 available FE J cases include elbows with circumferential/axial internal/external semi-elliptical surface cracks, axial internal extended surface cracks and fully-circumferential internal cracks under pressure, in-plane bending, out-of-plane bending, torsion and some combinations between two types of the four loads. The geometry, loading conditions and material properties for the 71 cases with semi-elliptical cracks are summarised in Lei and Budden (2022) and detailed information for the 4 cases with internal fully-circumferential or extended internal axial cracks can be found in Kayser (2016) or Lei (2020b). In the remainder of this paper, the cases from the “BENCH-KJ” report will be referred to as “BENCH-KJ” cases and the cases from the Frazer Nash report will be referred to as “FNC” cases.

Validation and Results

For each FE case, the FE J -based Option 3 FAC is constructed using Eqn. (11) below,

$$K_r(L_r) = \sqrt{(J_e)_{\text{est}}/J_{\text{FE}}} \quad (11)$$

where J_{FE} is the elastic-plastic total J value obtained from FE analyses for a given loading level, $(J_e)_{\text{est}}$ is the elastic J value, for the same loading level, estimated from SIF values obtained by following the recommended SIF estimation method described above and Eqn. (12) (R6 2019) below:

$$(J_e)_{\text{est}} = \frac{(1 - \nu^2)}{E} \left(K_I^2 + K_{II}^2 + \frac{K_{III}^2}{1 - \nu} \right) \quad (12)$$

where K_I , K_{II} and K_{III} are the SIF for mode I, II and III loading, respectively, and E and ν are Young's modulus and Poisson's ratio of the material, respectively. L_r in Eqn. (11) is evaluated via Eqn. (1) using the recommended limit load, global or local, for the same loading level. Note that the recommended global limit load solutions are very limited and only some of the cases are shown in the figures when global limit load is used. However, the local limit load applies for all the 75 cases. When using the recommended local limit load solution, stress correction has been applied to the cases which could be affected by plastic stress redistribution. This will be discussed further in Discussion below.

All the FE-based Option 3 data for "BENCH-KJ" cases are shown in Figs. 3 and 4 for circumferential and axial surface cracks, respectively, where both J_{FE} and $(J_e)_{\text{est}}$ are for the deepest point of the cracks (the maximum SIF and J are judged to be at the deepest point for surface cracks with $a/c \geq 1/3$). In each figure, the material stress-strain based Option 2 FAC is plotted, denoted by "OPT 2 (BENCH-KJ)". The R6 Option 1 FAC is also included, denoted as "OPT 1", in each figure for comparison.

From Figs. 3(a) and 4(a), for all circumferential/axial surface cracks under pressure or circumferential surface cracks under bending moment or combined moments, the Option 3 data points are located above the Option 2 FAC when the recommended global limit load solutions are used to define L_r . When L_r is defined using the recommended local limit load, from Figs. 3(b) and 4(b) for circumferential

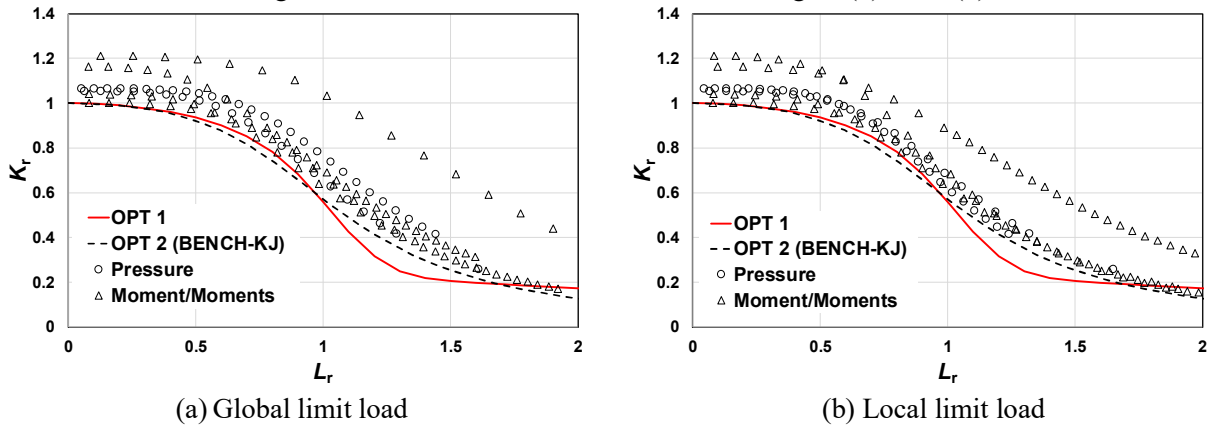


Figure 3 Comparison between the FE-based Option 3 curve and the Option 2 and Option 1 FACs "BENCH-KJ" cases of circumferential surface cracks

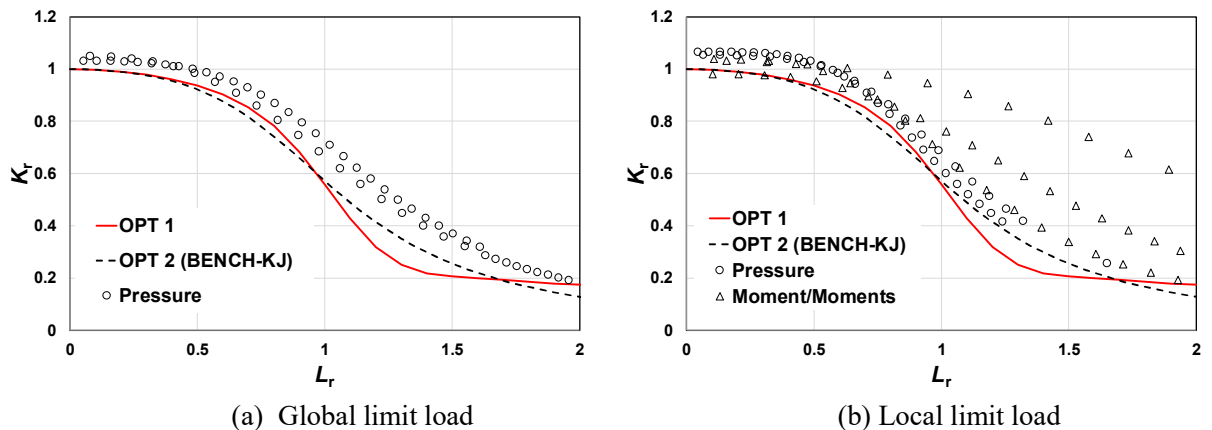


Figure 4 Comparison between the FE-based Option 3 curve and the Option 2 and Option 1 FACs "BENCH-KJ" cases of axial surface cracks

and axial surface cracks, respectively, the Option 3 data points are above the Option 2 FAC for all but one (see Fig. 4(b)) case. In Fig. 4(b), two data points for one case for an axial surface crack are slightly lower than the Option 2 FAC in the very low L_r region. This is because the SIF for this case is slightly underestimated. The overall results indicate that using recommended global/local limit load solutions and the SIF estimation method can lead to reasonably conservative assessment results for all the “BENCH-KJ” cases when the Option 2 FAC is used in the assessment.

It is seen from Figs. 3 and 4 that the Option 2 FAC for the material considered in the “BENCH-KJ” cases is slightly lower than the Option 1 FAC in the regions $0.5 < L_r < 0.9$ and $L_r > 1.7$. However, all the Option 3 data points are above the Option 1 FAC for $L_r < 1.7$. This means that the recommended global/local limit load solutions can also lead to conservative assessment results when the Option 1 FAC is used in assessments of the “BENCH-KJ” cases.

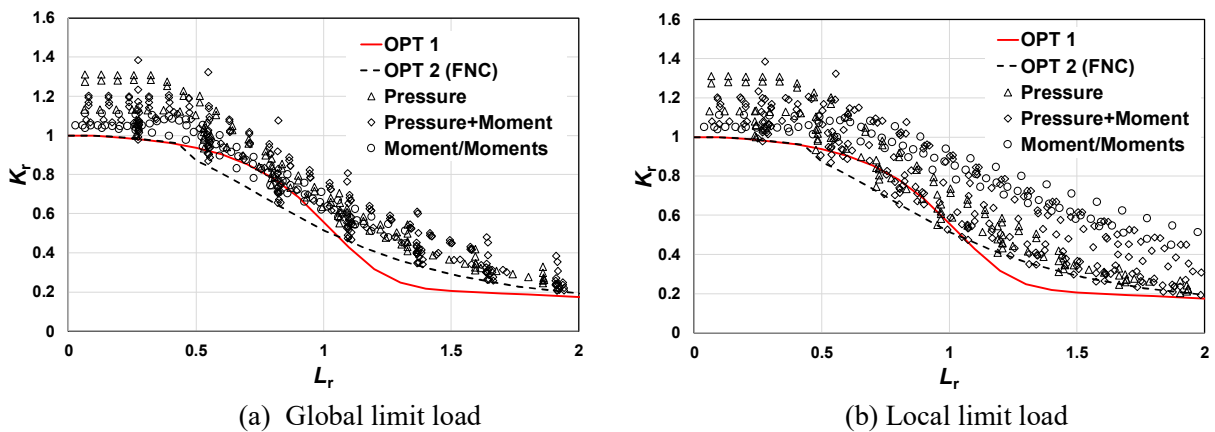


Figure 5 Comparison between the FE-based Option 3 curve and the Option 2 and Option 1 FACs “FNC” cases of circumferential surface cracks

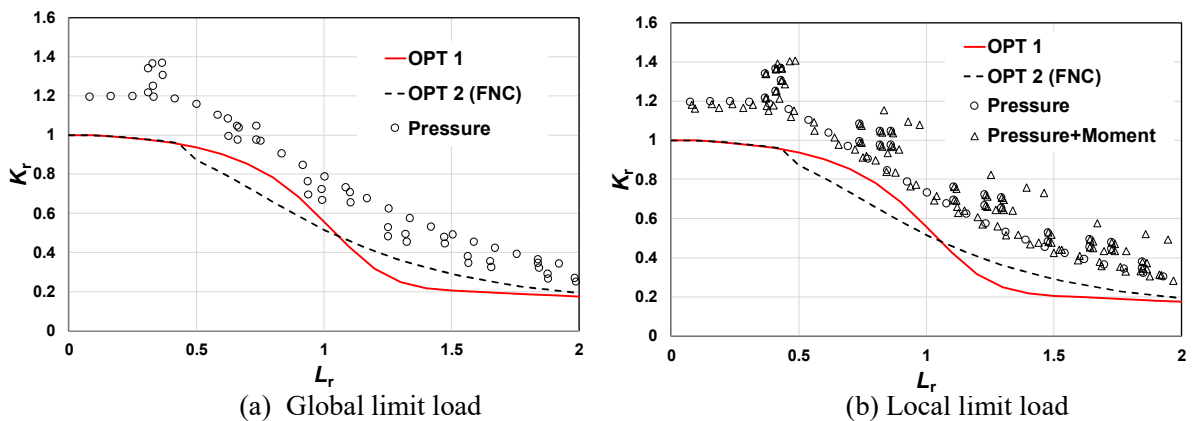


Figure 6 Comparison between the FE-based Option 3 curve and the Option 2 and Option 1 FACs “FNC” cases of axial surface cracks

All the FE-based Option 3 data for “FNC” cases are plotted in Figs. 5 and 6 for circumferential and axial surface cracks, respectively, against L_r defined by the recommended global and local limit load solutions, where J_{FE} is the maximum FE J obtained at the deepest or the near surface crack tip location and $(J_e)_{est}$ is the maximum elastic J estimated from the SIF values at the deepest or the surface point of the surface crack front. The material stress-strain curve based Option 2 FAC is plotted, denoted by “OPT 2 (FNC)”. Note that the material stress-strain curves used in the “FNC” Phase 1 and Phase 2 cases are slightly different (O’Neill and Brett (2016)). However, the Option 2 FACs for the two material stress-strain curves

are very close in the region $L_r < 2$. Therefore, “OPT 2 (FNC)” is used in the figures containing the cases from both Phase 1 and Phase 2 analyses. The R6 Option 1 FAC is also included, denoted as “OPT 1”, in each figure.

From Figs. 5(a) and 6(a), for all circumferential semi-elliptical surface cracks under pressure, combined pressure and a moment, or moments and for axial semi-elliptical surface cracks under pressure, respectively, the Option 3 data points for all cases are located above the Option 2 FAC when the recommended global limit load solutions are used to define L_r . When L_r is defined using the recommended local limit load, from Figs. 5(b) and 6(b), the Option 3 data points are above the Option 2 FAC for all cases. The results indicate that using recommended global/local limit load solutions and the SIF estimation method can lead to reasonably conservative assessment results for all the “FNC” cases when the Option 2 FAC is used in the assessments.

From Figs. 5 and 6, the Option 2 FAC for the material considered in the “FNC” cases is significantly lower than the Option 1 FAC in the region $0.45 < L_r < 1.05$. Some Option 3 data points in this region are below the Option 1 FAC in Fig. 5. This means that the recommended global/local limit load solutions may not lead to conservative assessment results for the “FNC” cases when the Option 1 FAC is used in the assessments.

DISCUSSION

Stress Intensity Factor Estimation

The SIF method recommended in the guidance was developed by Marie et al. (2007) for shallow surface cracks with $a/t \leq 0.25$. FE validation in Lei and Budden (2017) showed that using the recommended SIF method was conservative for deeper cracks.

For combined loading involving multi-load types, negative SIF values for some load types should be set to zero when calculating the total SIF value.

Global Limit Load Solutions

All the six global limit load solutions recommended in the guidance are “equivalent straight pipe solutions” developed in Lei (2021), based on the elbow pipe/crack geometry and loading similarity between an elbow and the corresponding straight pipe. The recommended solutions were validated in Lei (2021) using available elastic-perfectly plastic FE limit load results for various elbow/crack geometry parameters and load types. The results showed that this method provided conservative global limit load solutions for assessment of plastic collapse compared with FE limit load data. The FE J validation in Lei and Budden (2022) and in this paper show that using these global limit load solutions can lead to reasonably conservative fracture assessment results. If an elastic-perfectly plastic FE-based limit load needs to be used in a fracture assessment, elastic-plastic J validation should be provided.

Local Limit Load Solution

The recommended local limit load is based on the elastic through-thickness stress distributions at the crack location obtained from uncracked-body elastic stress analyses. Using elastic stresses leads to conservative assessment results, in general. However, in some locations, stress redistribution due to plastic deformation may occur and the elastic stresses may be lower than the real elastic-plastic stresses. In this case, using elastic stresses may lead to non-conservative assessment results and stress correction is required. In a pipe elbow, the area near the intersection between the elbow and the straight pipe is identified to be the site where plastic stress redistribution may occur and stress correction is required when evaluating the local limit load.

The guidance for stress correction is to carry out an elastic stress analysis for the uncracked straight pipe in addition to the elbow stress analysis. The maximum membrane stress normal to the crack plane from the two analyses should be used, together with other stress components from elastic elbow analysis, in evaluating the local limit load.

In Lei and Budden (2022), using the local limit load based on elastic stresses for the “BENCH-KJ” case CC-E-2 significantly underestimated the elastic-plastic FE J when used with the reference stress J estimation method. The “BENCH-KJ” CC-E-2 is a case for an internal circumferential semi-elliptical surface crack, located in the intersection between the elbow and straight pipe at the extrados, under in-plane closing bending. The FE J -based Option 3 curves are presented in Fig. 7. From the figure, the Option 3 data points are below the Option 2 FAC when L_r is defined by the local limit load based on the elbow elastic stresses (open triangles in the figure). However, when the stress correction is applied in evaluating the local limit load, which is then used to define L_r , the Option 3 data points (solid triangles) are all located above the Option 2 FAC.

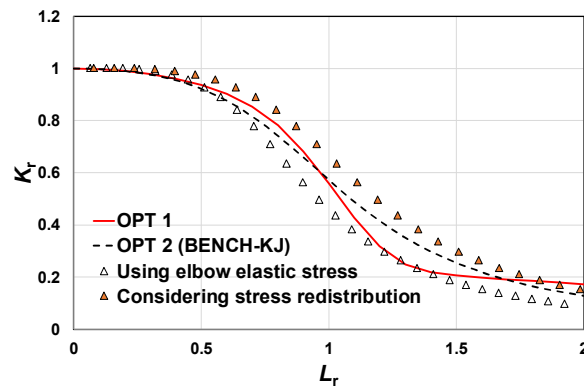


Figure 7 Correction of plastic stress redistribution when using local limit load (“BENCH-KJ” case CC-E-2)

Use of Option 1 FAC in Assessments

The validation in this paper shows that using the Option 1 FAC in R6 assessments can lead to conservative assessment results for the “BENCH-KJ” cases but may lead to non-conservative results for the “FNC” cases. This is because the Option 2 FACs for some materials may lie partly below the Option 1 FAC. The Option 1 FAC was originally derived as an approximate lower bound to Option 2 FACs for real stress-strain curves representative of a range of steels used in the UK nuclear industry. It was modified in R6 Revision 4, following the results of the European SINTAP project (SINTAP (1998)) where more steels used in other European countries were also considered, and is recommended for materials with continuous yielding. This means that using the Option 1 FAC in an assessment could lead to non-conservative results if the material stress-strain behaviour is very different from those considered in deriving the Option 1 FAC. For example, the Option 2 FAC of an idealised Ramberg-Osgood stress-strain curve with a low strain hardening index could be below the Option 1 FAC because of the large plastic strain when the stress is lower than the 0.2% proof stress. Therefore, sensitivity studies or validation should be carried out to show conservatism when using the Option 1 FAC in assessments for such materials.

CONCLUSIONS

This paper provides an overview of the newly-developed guidance for structural integrity assessment of defective pipe elbows using R6 and validation to support the new procedure. The guidance has been validated using 75 cases of 3-D finite element (FE) elastic-plastic J results, for smooth elbows of various geometries with axial/circumferential internal/external semi-elliptical/extended/fully-circumferential surface cracks under internal pressure, in-plane/out-of-plane bending moment, torsion and various load combinations, by comparing the FE-based Option 3 failure assessment curve (FAC) with the R6 Option 2 FAC. The results have shown that, for 74 out of 75 cases, the FE-based Option 3 curves are located above

the Option 2 FAC with reasonable conservatism when the guidance for using the elbow stress intensity factor and limit load was followed. In other words, following the newly-developed guidance can lead to reasonably conservative assessment results.

ACKNOWLEDGEMENT

The author wishes to acknowledge Dr P. J. Budden formerly of EDF Energy Nuclear Generation Ltd. for his valuable comments on this paper. This paper is published by permission of EDF Energy Nuclear Generation Ltd.

REFERENCES

- Kayser, Y. (2016). “BENCH KJ: overall synthesis of OECD benchmark activities”, CEA, Paris, France, Report No. DEN/DANS/DM2S/SEMT/LISN/NT/15-011/A.
- Lei, Y. (2017). “Stress intensity factors for defective pipe elbows”, EDF Energy Report E/REP/BBGB/0201/GEN/16 Revision 000. EDF Energy Nuclear Generation Ltd., Gloucestershire, UK.
- Lei, Y. (2020a). “Modification to a local limit load model to include the effect of bending stress parallel to the crack plane”, EDF Energy Report E/REP/BBGB/0240/GEN/20 Revision 000. EDF Energy Nuclear Generation Ltd., Gloucestershire, UK.
- Lei, Y. (2020b). “Validation of global/local limit load solutions of defective pipe elbows for use in structural integrity assessments”, EDF Energy Report E/REP/BBGB/0241/GEN/20 Revision 000. EDF Energy Nuclear Generation Ltd., Gloucestershire, UK.
- Lei, Y. (2021). “Review of limit load solutions for defective pipe bends”, EDF Energy Report E/REP/BBGB/0060/GEN/09 Revision 001. EDF Energy Nuclear Generation Ltd., Gloucestershire, UK.
- Lei, Y. and Budden, P. J. (2015). “Global limit load solutions for plates with surface cracks under combined biaxial forces and cross-thickness bending”, *International Journal of Pressure Vessels and Piping*, 132-133, 10-26.
- Lei, Y. and Budden, P. J. (2017). “Stress intensity factor estimation for defective pipe elbows”, SMiRT 24, Busan, Korea - August 20-25, 2017.
- Lei, Y. and Budden, P. J. (2022). “J predictions for defective pipe elbows via the reference stress method”, *Journal of Pressure Vessel Technology*, 144(3): 031303.
- Marie, S., Chapuliot, S., Kayser, Y., Lacire, M. H., Drubay, B., Barthelet, B., Le Delliou, P., Rougier, V., Naudin, C., Gilles, P. and Triay, M. (2007). “French RSE-M and RCC-MR code appendices for flaw analysis: Presentation of the fracture parameters calculation—Part IV: Cracked elbows”, *International Journal of Pressure Vessels and Piping*, 84 659–686.
- O'Neill, J. and Brett, A. (2016). “Defects in welds adjacent to elbows—Review of reference stress solutions,” Frazer-Nash Consultancy, Dorking, Surrey, UK, Report No. FNC 47710/43527R Issue 1.
- R6 (2019). “Assessment of the Integrity of Structures Containing Defects”, Revision 4, Amendment 12, EDF Energy Nuclear Generation Ltd., Gloucestershire, UK.
- SINTAP (1998). Structural Integrity Assessment Procedures for European Industry, Final Procedure, British Steel Report.